Ionics (2017) 23:2185–2191
DOI 10.1007/s11581-017-2050-9

ORIGINAL PAPER

Three-dimensional graphene nanosheets supported by NiO/Si-MCP as electrode materials for high-performance supercapacitors

Bairui Tao[1] · Hui Shao[1] · Jianbo Yu[2] · Rui Miao[1] · Zaishun Jin[2] · Fang Liu[2] · Paul K. Chu[3] · Zhin-Bin Zhang[4] · Fengjuan Miao[1]

Received: 22 January 2017 / Revised: 18 February 2017 / Accepted: 24 February 2017 / Published online: 14 March 2017

Abstract A three-dimensional (3D) graphene/NiO/Si-microchannel (MCP) composite electrode is synthesized by the conventional microelectronic machining process and electrochemical exfoliation technology for electrochemical capacitors. SEM, AFM, and Raman scattering are used to investigate the morphology and structure, and electrochemical characterization reveals that the 3D graphene/NiO/Si-MCP has a high specific capacitance of 833 Fg^{-1} at a current density of 5 Ag^{-1} in 6 mol L^{-1} KOH. Moreover, good cycling performance with 92% capacitance retention after 1000 cycles is observed indicating the novel electrode has large potential in high-performance supercapacitors.

Keywords Graphene/NiO/Si-MCP · Electrochemical exfoliation · Supercapacitors

Introduction

Graphene, a two-dimensional structure with a single layer of honeycomb sp^2 carbon lattice, has received tremendous attention in energy storage devices such as Li–ion batteries and supercapacitors due to the excellent conductivity, large surface-to-volume ratio, and good electrochemical stability [1–5]. Several methods have been employed to prepare graphene, for example, mechanical exfoliation [6], epitaxy [7], chemical vapor deposition (CVD) [8, 9], and electrochemical exfoliation [10–13]. Although electrochemical exfoliation is an easy, fast, and environmentally friendly method to produce high-quality graphene, agglomeration of adjacent graphene sheets occurs because of the strong π–π interaction. Graphene sheets have been integrated with other materials such as polymers and by self-assembly into various macroscopic structures to alleviate the aforementioned problems. Chen et al. incorporated two-dimensional (2D) graphene sheets into macroscopic structures to produce 3D foam-like graphene macrostructures with good electrical and mechanical properties [14], and Wu et al. synthesized 3D thermally reduced graphene on Ni foam and the materials had high specific capacitance [5]. Xu et al. prepared a self-assembled graphene hydrogel by a convenient one-step hydrothermal method, and the product is electrically conductive, mechanically strong, and thermally stable and also has a high specific capacitance [15]. However, research on graphene made by electrochemical exfoliation of graphite with silicon for integrated circuits is quite scarce [16–19].

In this work, 3D graphene nanosheets are produced on nickel oxide-coated silicon microchannel (NiO–Si/MCP) and the application to supercapacitors is evaluated. The silicon microchannel (Si-MCP) having a macroporous structure and ordered channel is better than most conventional porous materials and constitutes an important class of electrode materials in electrochemical devices [20]. Modification of the Si-MCP inner wall with better electrode materials can improve the capacitive behavior, and so, it is possible to form an electrode for high-performance supercapacitors.

✉ Bairui Tao
tbr_sir@163.com

✉ Fengjuan Miao
miaofengjuan@163.com

[1] College of Communications and Electronics Engineering, Qiqihar University, Qiqihar, Heilongjiang 161006, China

[2] Mudanjiang Medical College, Qiqihar, Heilongjiang 157011, China

[3] Department of Physics and Materials Sciences, City University of Hong Kong, Tat Chee Avenue, Kowloon, Hong Kong, China

[4] Solid State Electronics, Ångströmlaboratoriet, Uppsala University, SE-75121 Uppsala, Sweden

Experimental details

Few-layer graphene preparation by electrochemical exfoliation

Electrochemical exfoliation of few-layer graphene was performed in a two-electrode system. A platinum (Pt) wire was used as the counter electrode, and a graphite rod served as the working electrode. The two electrodes were placed in parallel with a separation of 3.0 cm. $(NH_4)_2SO_4$ (0.1 M) was the electrolyte to which a voltage of +5 V was applied for 20 min. Afterwards, the exfoliated product was collected by vacuum filtration and rinsed repeatedly. The powder was added to 20 mL of ethanol and sonicated for 20 min [21].

Fabrication of NiO/Si-MCP support

The Si-MCP was synthesized by a method described previously [22–24]. P-type <100> silicon with resistivity of 2–8 Ω cm was the substrate in Si-MCP fabrication which consisted of five main steps: (i) A 300-nm thick SiO_2 layer was thermally grown on the substrate as a mask, (ii) proper square regions were formed on the mask surface by photolithography and etched in buffered hydrofluoric acid, (iii) pyramidal notches were created in a tetramethylammonium hydroxide solution prior to anodizing, (iv) the SiO_2 layer was removed, and (v) photo-assisted electrochemical etching was performed to produce the 3D ordered Si-MCP.

Electroless plating was used to produce the Ni film on the Si-MCP. The separated Si-MCPs were segmented into small chips with a rectangular shape. After a standard RCA cleaning process, the samples were put in a buffer solution (Triton X-100) for 30 s to decrease the inner stress and enhance wetting before immersing in a plating bath for 30 min at 70 °C. Afterwards, they were taken out and rinsed with water and annealed at 300 °C for 300 s under oxygen in a rapid thermal annealing (RTA) system to synthesize NiO nanostructures on the sidewalls of the MCP. The plating solution was prepared with nickel sulfate ($NiSO_4$), ammonium sulfate ($(NH_4)_2SO_4$), nickel sulfate (NH_4F), sodium citrate ($C_6H_5Na_3O_7$), sodium lauryl sulfate ($CH_3(CH_2)_{10}CH_2OSO_3Na$), and deionized water, and the pH was adjusted to 8.0 with ammonia during plating.

Preparation of three-dimensional graphene nanosheets on NiO/Si-MCP

After drying under flowing nitrogen, the few-layer graphene was deposited by electrophoresis in a solution on the NiO/Si-MCP in a solution for different time durations. The nanocomposite was dried at 180 °C for 200 s in air to enhance the stability. The samples were designated as graphene/NiO/Si-MCP-*x*, where *x* referred to the mass of graphene on the NiO/Si-MCP (mg cm^{-2}). Copper wires were connected to the silver conductive adhesive to facilitate subsequent electrochemical experiments. The fabrication process is shown in Fig. 1.

Characterization

The morphology of the few-layer graphene and graphene/NiO/Si-MCP was examined by scanning electron microscopy (SEM). Raman scattering was carried out on a LabRAM HR800 Raman spectrometer with a laser wavelength at 532 nm, and X-ray photoelectron spectroscopy (XPS) was conducted on a Genesis X-ray energy-dispersive spectrometer to determine the chemical states and composition. Electrochemical characterization was carried out in a conventional three-electrode cell with 6 M KOH as the electrolyte. A platinum foil and saturated calomel electrode (SCE) were used as the counter and reference electrodes, respectively, and all the electrochemical measurements were performed on an electrochemical workstation.

Results and discussion

Morphology of the graphene/NiO/Si-MCP nanocomposite

The structure and morphology of the products are analyzed by SEM, atomic force microscopy (AFM), XPS, and Raman scattering. Figure 2a, b displays the top and cross-sectional views of the Si-MCP revealing regular squares. The hole size is defined by photolithography. There are little impurities in each channel, and all the channels are aligned orderly. By controlling the etching time, etchant, and temperature, both the length and the width can be varied. In our experiments, the length of the channels is approximately 200 μm. The Si-MCP is a transparent and connective film which is lifted off from the silicon substrate. Figure 2c depicts the SEM picture of graphene flakes with different size on the silicon wafer. One hundred graphene nanosheets are randomly selected and measured by AFM. Figure 2d shows the representative AFM image and statistical thickness distribution of the graphene nanosheets. The thickness of 80 graphene nanosheets is less than 3 nm, and so, the percentage of graphene nanosheets with a layer number of <5 is 80%. Based on the statistical analysis, the number of layers in the graphene nanosheets is 2–4 and the lateral size is between 50 and 650 nm. Figure 2e shows are three Raman peaks at 1350, 1580, and 2710 cm^{-1} corresponding to the D, G, and 2D peaks, respectively. The results show a significant change in the relative intensity of the 2D band and G band of graphene compared to pristine graphite. The ratio of the intensity of the D peak to G peak can be employed to characterize the defect concentration in graphene. Here, I_D/I_G is 1.21 indicating a large amount of defects [25].

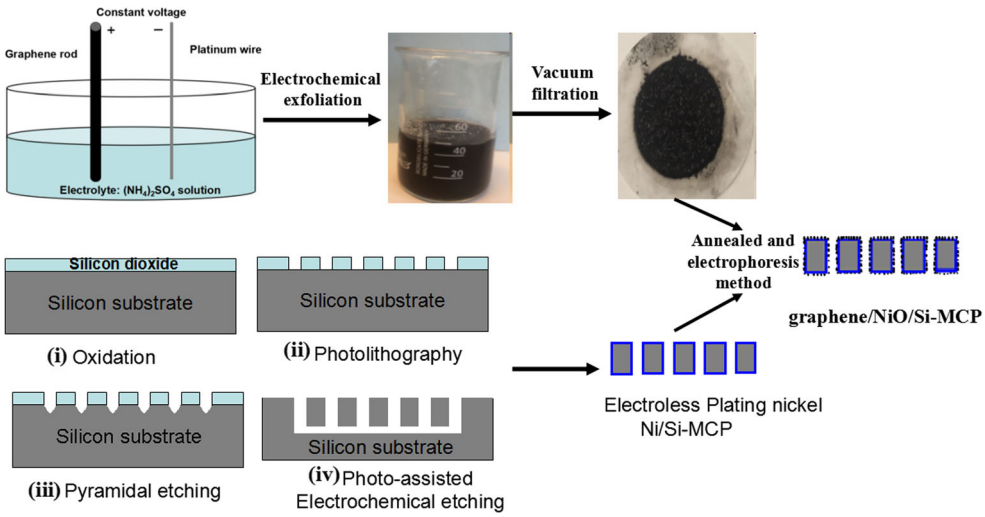

Fig. 1 Fabrication process of the three-dimensional graphene nanosheets supported by the NiO/Si-MCP electrode

Figure 3a–d shows the top and cross-sectional views of the NiO/Si-MCP and graphene/NiO/Si-MCP nanocomposites. The NiO/Si-MCP and graphene/NiO/Si-MCP have a regular square morphology with aligned and channels. The channels are still uniformly distributed, isolated, and parallel to each other after electroless deposition Ni. The nickel film on the inner walls of the Si-MCP serves as both the current collector layer and the protection layer. The nickel layer is not smooth thus providing a larger surface area to form nickel hydroxide. The graphene sheets adhere well to the surface, and the channel of the NiO/Si-MCP is shown in Fig. 3c, d. By controlling the electrophoresis time and concentration of graphene, the length and width of each channel can be tailored. The EDS results in Fig. 3f show that the composite mainly consist of C, Ni, and O. No characteristic peaks of Si can be found, confirming that the layer covers the surface of Si entirely.

As shown by the survey XPS spectrum of graphene/NiO/Si-MCP in Fig. 4, C1s and O1s signals are observed at 284 and 530 eV. The few-layer graphene nanosheets have an O/C atomic ratio of about 0.23. The high-resolution C1s spectrum can be deconvoluted into three Gaussian peaks at 284.1, 285.5, and 288.0 eV corresponding to sp^2 C (C–C, C=C), sp^3 C (C–O), and oxidized C (C=O), respectively [26]. The strong C=C signal indicates good graphitization of graphene, and the oxygen-containing characteristic of graphene enhances the wettability in subsequent application. The spectra

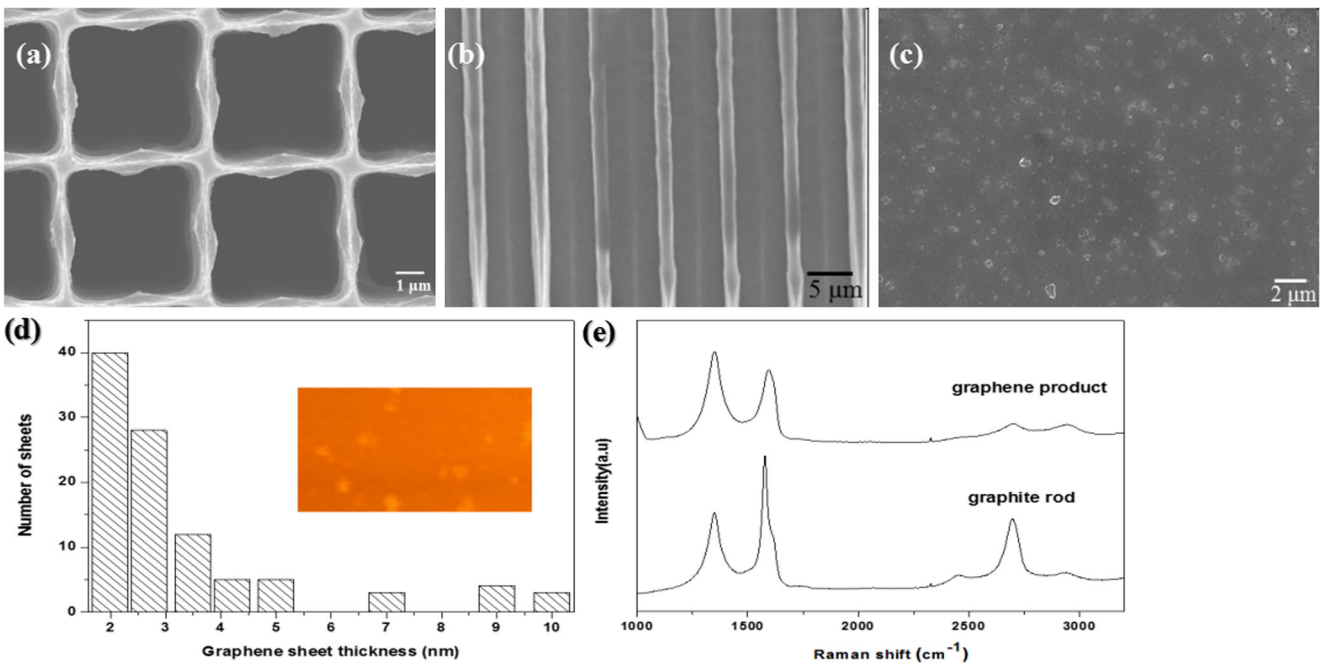

Fig. 2 **a** Top-view SEM image of the microstructure of Si-MCP. **b** Cross-sectional SEM image of the microstructure of the Si-MCP. **c** SEM image of graphene flakes on the silicon wafer. **d** Statistical thickness distribution histogram of the graphene nanosheets measured by AFM (*inset* showing a typical AFM image). **e** Raman scattering results of graphene flakes

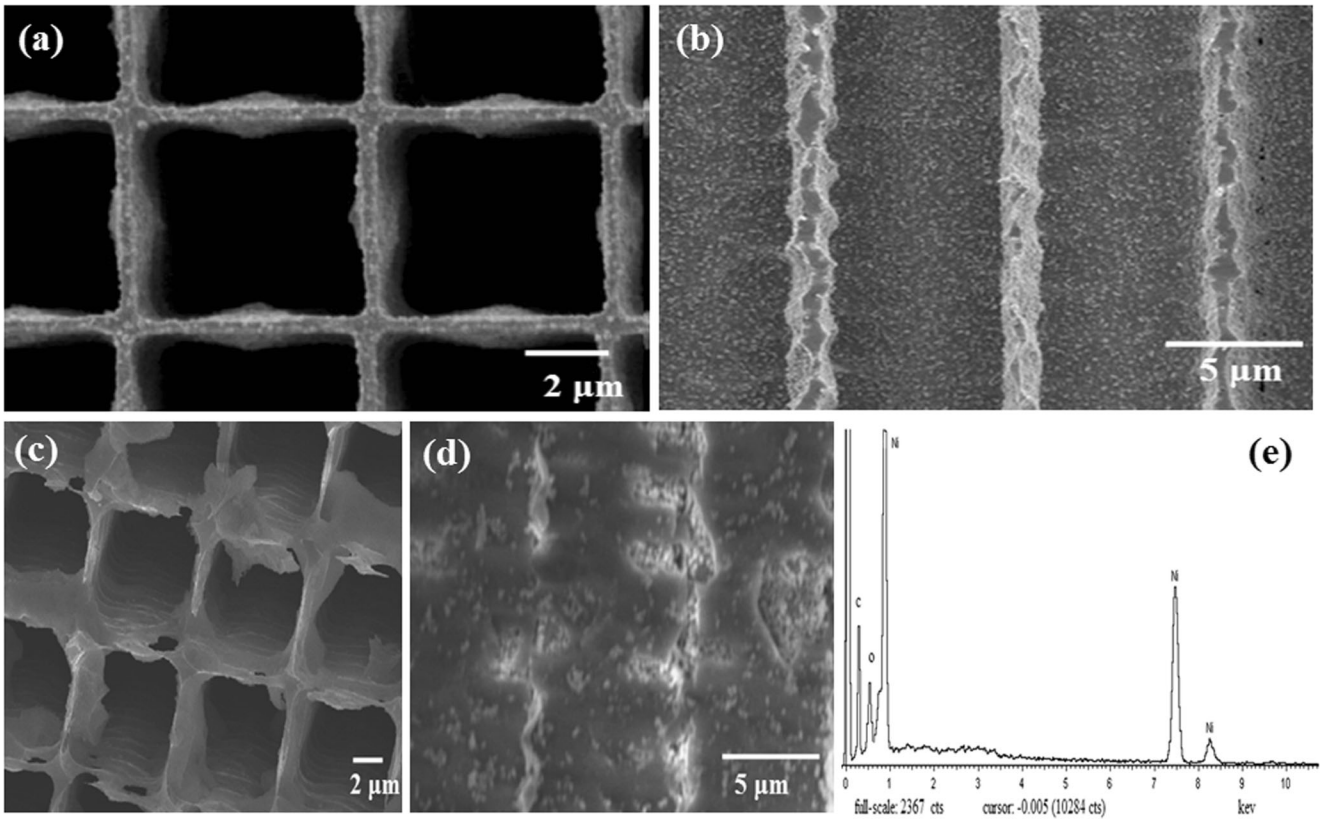

Fig. 3 Top and cross-sectional SEM images of **a**, **b** NiO/Si-MCP, **c**, **d** graphene/NiO/Si-MCP and **e** the EDS result of graphene/NiO/Si-MCP

clearly reveal that the intrinsic in-plane crystal structure of graphite remains intact after electrochemical exfoliation.

To evaluate the electrochemical performance of the graphene/NiO/Si-MCP electrode, cyclic voltammetry (CV) is performed in 6 mol L^{-1} KOH using a three-electrode system. For comparison, NiO/Si and NiO/Si-MCP are prepared by the same procedures. Figure 5 shows the CV curves of NiO/Si, NiO/Si-MCP, and graphene/NiO/Si-MCP at a scanning rate of 50 mV^{-1} revealing a pair of typical oxidation and reduction peaks caused by the following reversible electrochemical reaction: $Ni^{2+} + 2OH^- \rightarrow Ni(OH)_2$, $Ni(OH)_2 + OH^- \rightarrow NiOOH + H_2O + e^-$ [27]. The current density of NiO/Si-MCP is greater than that of NiO/Si. After graphene deposition, the capacitive characteristics such as the current density and peak positions of the NiO/Si-MCP electrode are different. The CV curve of the graphene/NiO/Si-MCP is nearly a horizontal line along the potential axis, whereas the graphene/NiO/Si-MCP shows a pair of redox peaks with a large current,

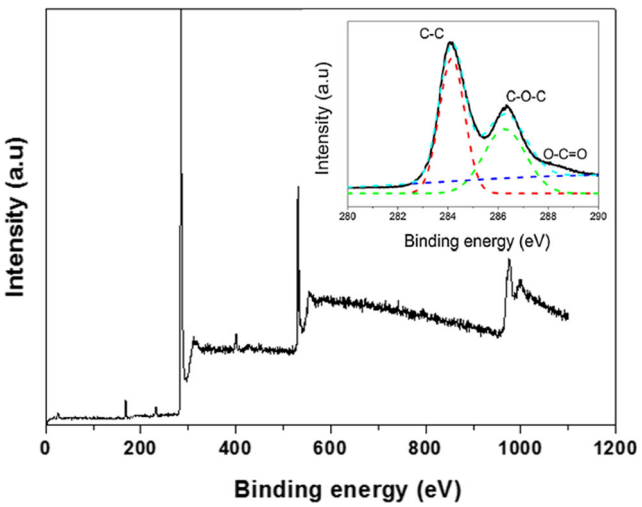

Fig. 4 X-ray photoelectron spectroscopy (XPS) results of graphene/NiO/Si-MCP

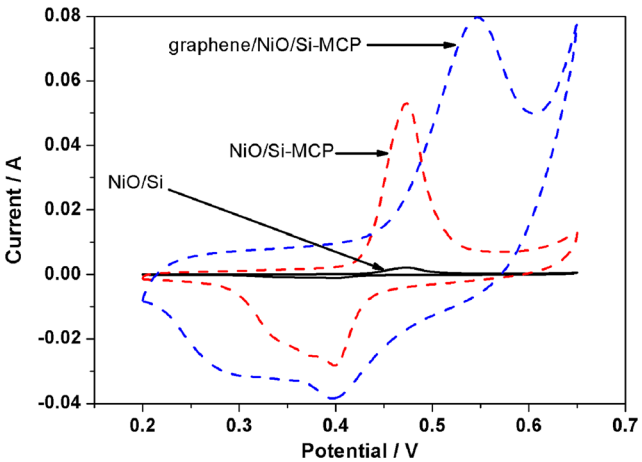

Fig. 5 Cyclic voltammograms of *NiO/Si*, *NiO/Si-MC*, and *graphene/NiO/Si-MCP* at a scanning rate of 50 mV^{-1}

indicating that graphene contributes significantly to the specific capacitance.

The covered area on the NiO/Si-MCP is larger than that on NiO/Si, implying a large specific capacitance associated with the Si-MCP supporter. Each curve shows a roughly mirror image with respect to the zero-current line. At each end potential, the electrodes show a rapid current response on potential reversal indicating excellent electrochemical activity, high power density, and a capacitive behavior.

Figure 6a shows the CVs of graphene/NiO/Si-MCP-x ($0 \leqq x \leqq 1$ at intervals of 0.2 mg) with different concentrations of graphene. They show a pair of well-defined redox peaks in the chosen voltage range. When the graphene content is increased, the covered area in the CV curve is larger implying higher capacitance. However, when the graphene concentration exceeds the threshold of $x = 1.4$, the capacitance decreases. The specific capacitance is calculated by the following equation: $C = \int \frac{IdV}{mv(\Delta V)}$, where $\Delta V$is the electrochemical window, I (A) is the respond current, v (Vs^{-1}) is the scanning rate, and m (g) is the mass of the active electrode materials. Graphene/NiO/Si-MCP-1.4 exhibits a high capacitance of 924 Fg^{-1} due to the following reasons: (1) high specific surface area and ordered channels in the Si-MCP structure leading to more effective active materials and high charge transfer rate between the electrolyte and the electrode; (2) formation of $Ni(OH)_2$ in the reaction which provides a high pseudocapacitance; and (3) good characteristics of few-layer graphene, especially the large concentration of oxygen functional groups on graphene which can provide high pseudocapacitance as shown in Eqs. (1)–(3)

$$> C\text{–}OH \leftrightharpoons > C = O + H^+ + e^- \quad (1)$$

$$-COOH \leftrightharpoons -COO + H^+ + e^- \quad (2)$$

$$> C = O + e^- \leftrightharpoons > C\text{–}O^- \quad (3)$$

The CVs of graphene/NiO/Si-MCP-1.4 electrode at different sweeping rates are shown in Fig. 6b. The area under the CV curves increases with scanning rates, but the anodic and cathodic peaks shift towards positive and negative potentials, respectively, demonstrating the quasi-reversible nature of the redox reactions [28]. When the seeping rate reaches 100 mV s^{-1}, the CV curve of the graphene/NiO/Si-MCP-1.4 electrode remains changed indicative of a perfect supercapacitor behavior.

Figure 7 shows the results of the galvanostatic charge/discharge cycling experiments obtained from the graphene/NiO/Si-MCP-1.4 capacitor. The current density is 5 Ag^{-1}, and the discharging time for each cycle is about 100 s. The curves show some deviations from the ideal triangular shape due to the pseudocapacitance. The specific capacitance can be calculated by the equation $C = I \times \Delta t/(m \times \Delta V)$, where C (Fg^{-1})

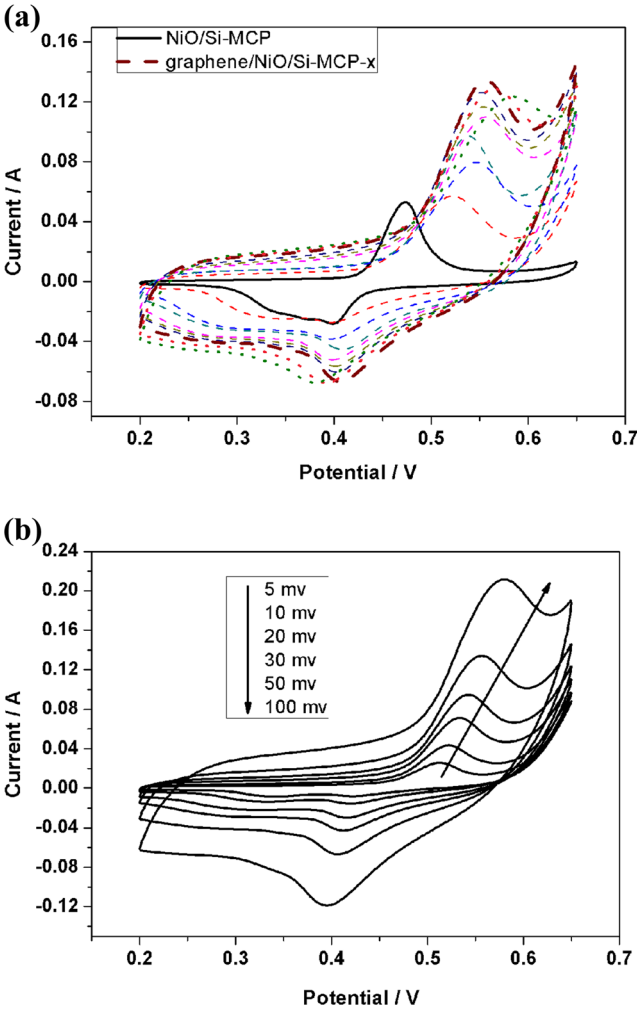

Fig. 6 **a** CVs of the graphene/NiO/Si-MCP-x electrodes with various concentrations of graphene. **b** CVs of graphene/NiO/Si-MCP-1.4 at different sweeping rates

is the specific capacitance of the electrode, I (A) is the discharge current, Δt (s) is the discharge time, m (g) refers to the mass of

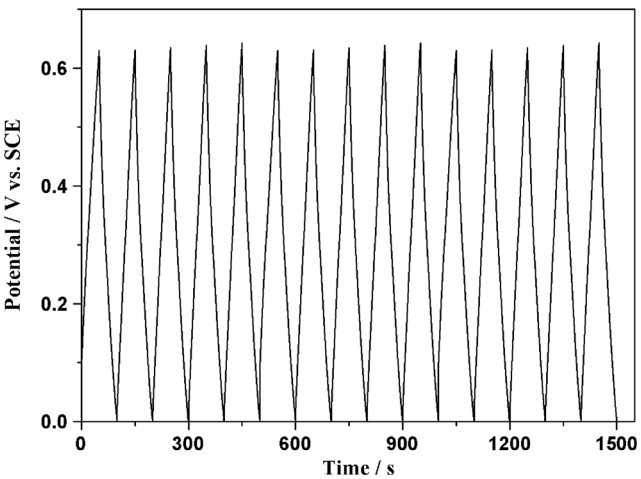

Fig. 7 Charging–discharging behavior of the graphene/NiO/Si-MCP-1.4 electrode at a current density of 5 Ag^{-1}

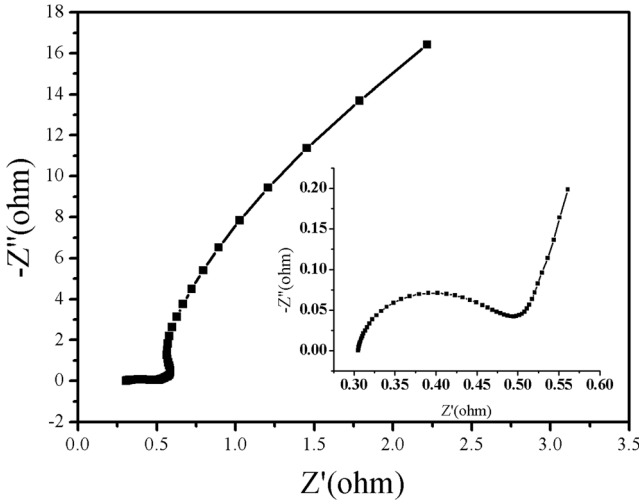

Fig. 8 EIS spectra of the graphene/NiO/Si-MCP electrode

the active materials, and ΔV (V) is the potential window in the cycling test. The largest capacitance achieved is 833 Fg^{-1}.

The outstanding rate capability of the graphene/NiO/Si-MCP electrode may be attributed to the 3D and highly connected structure with good electron and ion transport capability. The 3D framework structure provides ordered channels for electron conduction, and the framework in graphene/NiO/Si-MCP provides more ion-buffering reservoirs and transport pathways to decrease the distance for ion transport thereby facilitating diffusion of the electrolyte ions.

To further evaluate the electrochemical and structural characteristics of the graphene/NiO/Si-MCP-1.4 electrode, the impedance spectra are analyzed using the Nyquist plots by applying an AC voltage with a 5-mV amplitude in a frequency range from 0.1 Hz to 100 kHz. The imaginary component of the impedance against the real component is shown in Fig. 8. The semicircle at higher frequencies corresponds to the charge transfer resistance (Rct) caused by the Faradaic reaction and double layer capacitance (Cdl) at the interface between the electrode and the electrolyte solution [29]. The diameter of the semicircle of graphene/NiO/Si-MCP is very small reflecting low charge transfer and electrolyte resistance. The vertical line in the Nyquist plot of graphene/NiO/Si-MCP at lower frequencies is almost parallel to the imaginary axis suggesting a good capacitive behavior and that graphene/NiO/Si-MCP provides shorter diffusion paths to improve the charge transfer performance.

The cycling stability of the graphene/NiO/Si-MCP electrode is investigated by charging/discharging tests performed at a current density of 5 Ag^{-1}. As shown in Fig. 9, although the specific capacitance decreases with cycle numbers, the specific capacitance is 766 Fg^{-1} after 1000 cycles corresponding to 92% capacity retention.

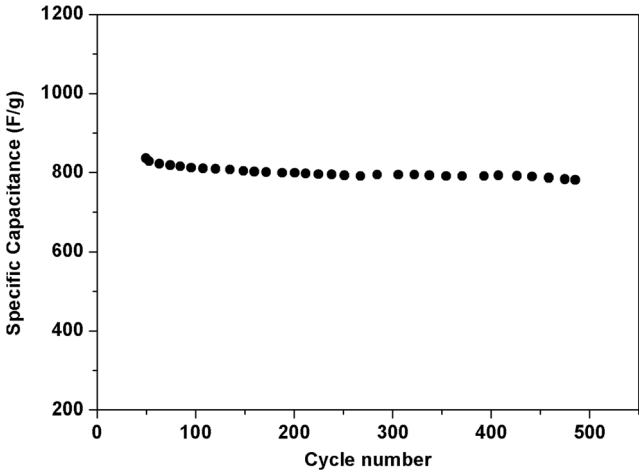

Fig. 9 Cyclic stability of the graphene/NiO/Si-MCP electrode determined by charging/discharging tests conducted at a current density of 5 Ag^{-1}

Conclusion

A novel graphene/NiO/Si-MCP nanocomposite is fabricated for supercapacitor electrodes. The Si-MCP array serves as the backbone, and the fabrication procedures are compatible with microelectronics processing. The materials which have a large specific area for loading active graphene exhibit very high specific capacitance and good stability. The structure is easily integratable with microelectronic devise and has promising potential in high-performance supercapacitors.

Acknowledgements This work was jointly supported by the National Natural Science Foundation of China (Grant Nos. 61204127, 81172204, and 81271628), Natural Science Foundation of Heilongjiang Province (Grant Nos. F201332 and F201438), New Century Excellent Talents in Heilongjiang Provincial University (Grant No. 1253-NECT025), Science and Technology Project of Qiqihar (Grant GYGG-201409), postdoctoral scientific research developmental fund of Heilongjiang Province (Grant No. LBH-Q15142 and LBH-Q14157), higher school science and technology achievements industrialization pre-research and development foundation of Heilongjiang Province (Grant No. 1254CGZH04), and City University of Hong Kong Applied Research (Grant (ARG) No. 9667122).

References

1. Fan Z, Yan J, Zhi L, Zhang Q, Wei T, Feng J et al (2010) A three dimensional carbon nanotube/graphene sandwich and its application as electrode in supercapacitors. Adv Mater 22(33):3723–3728
2. Xie KY, Wei BQ (2014) Materials and structures for stretchable energy storage and conversion devices. Adv Mater 26(22):3592–3617
3. Du X, Guo P, Song H, Chen X (2010) Graphene nanosheets as electrode material for electric double-layer capacitors. Electrochim Acta 55(16):4812–4819
4. Huang Y, Liang J, Chen Y (2012) An overview of the applications of graphene-based materials in supercapacitors. Small 8(12):1805–1834

5. Wu XL, Yang D, Wang CK, Jiang YT, Wei T, Fan ZJ (2015) Functionalized three-dimensional graphene networks for high performance supercapacitors. Carbon 92:26–30
6. Chen J, Duan M, Chen G (2012) Continuous mechanical exfoliation of graphene sheets via three-roll mill. J Mater Chem 22:19625–19628
7. Heer WA, Berger C, Wu XS et al (2007) Epitaxial graphene. Solid State Commun 143:92–100
8. Sutter PW, Flege JI, Sutter EA (2008) Epitaxial graphene on ruthenium. Nat Mater 7:406
9. Lee Y, Bae S, Jang H, Jang S, Zhu SE, Sim SH, Song YI, Hong BH, Ahn JH (2010) Wafer-scale synthesis and transfer of graphene films. Nano Lett 10:490
10. Parvez K, Li RJ, Puniredd SR, Hernandez Y, Hinkel F, Wang SH, Feng XL, Müllen K (2013) Electrochemically exfoliated graphene as solution-processable, highly conductive electrodes for organic electronics. ACS Nano 7:3598
11. Lee JH, Shin DW, Makotchenko VG, Nazarov AS, Fedorov VE, Kim YH, Choi JY, Kim JM, Yoo JB (2009) One-step exfoliation synthesis of easily soluble graphite and transparent conducting graphene sheets. AdvMater 21:4383
12. Liu N, Luo F, Wu HX, Liu YH, Zhang C, Chen J (2008) One-step ionic-liquid-assisted electrochemical synthesis of ionic-liquid-functionalized graphene sheets directly from graphite. Adv Funct Mater 18:1518
13. Su CY, Lu AY, Xu YP, Chen FR, Khlobystov AN, Li LJ (2011) High-quality thin graphene films from fast electrochemical exfoliation. ACS Nano 5:2332
14. Chen ZP, Ren WC, Gao LB, Liu BL, Pei SF, Cheng HM (2011) Three-dimensional flexible and conductive interconnected graphene networks grown by chemical vapour deposition. Nat Mater 10:424–428
15. Xu Y, Sheng K, Li C, Shi G (2010) Self-assembled graphene hydrogel via one-step hydrothermal process. ACS Nano 4:4324–4330
16. An L, Xu K, Li W, Liu Q, Li B, Zou R, Chen Z, Hu J (2014) Exceptional pseudocapacitive properties of hierarchical NiO ultrafine nanowires grown on mesoporous NiO nanosheets. J Mater Chem A 2(32):12799–12804
17. Zhang GQ, Yu L, Hoster HE, Lou XW (2013) Synthesis of one-dimensional hierarchical NiO hollow nanostructures with enhanced supercapacitive performance. Nano 5(3):877–881
18. Wang B, Chen JS, Wang ZY, Madhavi S, Lou XW (2012) Green synthesis of NiO nanobelts with exceptional pseudo-capacitive properties. Adv Energy Mater 2:1188–1192
19. Ding SJ, Zhu T, Chen JS, Wang ZY, Yuan CL, Lou XW (2011) Controlled synthesis of hierarchical NiO nanosheet hollow spheres with enhanced supercapacitive performance. J Mater Chem 21:6602–6606
20. Miao FJ, Tao BR, Ci PL, Shi J, Wang LW (2009) 3D ordered NiO/silicon MCP array electrode materials for electrochemical supercapacitors. Mater Res Bull 44:1920–1925
21. Parvez K, Wu ZS, Li RJ, Liu X, Graf R, Feng XL, Müllen K (2014) Exfoliation of graphite into graphene in aqueous solutions of inorganic salts. J Am Chem Soc 136:6083–6091
22. Chen XM, Lin JL, Yuan D, Ci PL, Xin PS, Xu SH, Wang LW (2008) Obtaining a high area ratio free-standing silicon microchannel plate via a modified electrochemical procedure. J Micromech Microeng 18(3):037003
23. Tao B, Zhang J, Miao F et al (2010) Preparation and electrochemistry of NiO/SiNW nanocomposite electrodes for electrochemical capacitors [J]. Electrochim Acta 55(18):5258–5262
24. Morimoto T, Hiratsuka K, Sanada Y et al (1997) Electric double-layer capacitor using organic electrolyte [J]. J Power Sources 60(2):239–247
25. Chabot V, Kim B, Sloper B, Tzoganakis C, Yu A (2013) High yield production and purification of few layer graphene by gum arabic assisted physical sonication. Scientific reports 3:1378–1385
26. Laszlo K, Tombacz E, Josepovits K (2001) Effect of activation on the surface chemistry of carbons from polymer precursors. Carbon 39:1217–1228
27. Cai FS, Zhang GY, Chen J, Gou XL, Liu HK, Dou SX (2004) $Ni(OH)_2$ tubes with mesoscale dimensions as positive-electrode materials of alkaline rechargeable batteries. Angew Chem 434:212
28. Dubal DP, Gund GS, Holze R, Jadhav HS, Lokhande CD, Park C (2013) Surfactant-assisted morphological tuning of hierarchical CuO thin films for electrochemical supercapacitors. Dalton Trans 42:6459
29. Barsoukov E, Macdonald JR (Eds) (2005) Impedance spectroscopy—theory, experiment, and applications. Wiley-Interscience. doi: 10.1002/0471716243